Synthesis, Characterization, and Stability of Poly[(alkylene oxide) ester] Thermoplastic Elastomers

SIMON J. MCCARTHY, GORDON F. MEIJS, PATHIRAJA GUNATILLAKE

CSIRO Division of Chemicals and Polymers, Private Bag 10, Clayton South MDC, Victoria 3169, Australia

Received 13 August 1996; accepted 16 January 1997

ABSTRACT: Poly(ether ester) block copolymers were prepared using a transesterification/polycondensation bulk synthesis with systematic control of the terephthalic acid/butanediol aromatic diester block ('hard segment') and with poly(tetramethylene oxide) [PTMO], poly(hexamethylene oxide) [PHMO], or poly(decamethylene oxide) [PDMO] poly(alkylene oxide) soft segments. The respective number average molecular weights were 980, 930, and 940 Da. A series of the poly(ether ester)s with hard segment fractions of 25, 29, 37, and 51% were prepared. One example of the PDMO polyester was prepared at a 51% hard segment fraction. The polyesters were characterized using viscometry, gel permeation chromatography, ^{1}H-NMR spectroscopy, differential scanning calorimetry, and tensile testing. The novel poly(ether ester)s, the PTMO polyester, and the commercial control, Hytrel® 4056, were compared for their resistance to degradation in a 50% aqueous hydrogen peroxide solution at 37°C, boiling water buffered at pH 1 and 13, an oxygen stream at 200°C, and a nitrogen stream at 200°C. The Hytrel® 4056 and the PTMO polyesters fragmented in hydrogen peroxide within 24 h while the PHMO and PDMO polyesters were much less degraded. Resistance to hydrolytic and thermal degradation increased as the ratio of aliphatic methylene to ether increased: PTMO < PHMO < PDMO. Samples containing higher hard segment fractions demonstrated improved resistance to hydrolysis.
 J Appl Polym Sci **65:** 1319–1332, 1997

Key words: poly[(alkylene oxide) ester]; thermoplastic elastomer; degradation; poly(tetramethylene oxide); poly(hexamethylene oxide); poly(decamethylene oxide)

INTRODUCTION

Poly(ether ester) segmented thermoplastic elastomers, typified by the terephthalic acid/butanediol poly(ether ester) (**I**), combine the mechanical properties of high performance elastomers and flexible plastics.

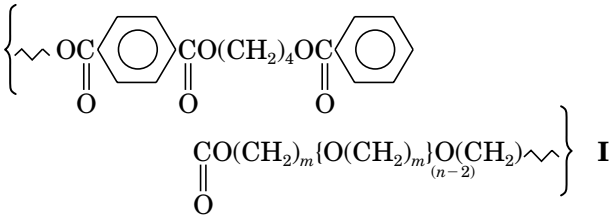

I

Correspondence to: S. J. McCarthy.
 CCC 0021-8995/97/071319-14

They are known for exceptional toughness and resilience and their high resistance to creep, impact, and flex fatigue. They also have good flexibility at low temperatures[1,2] and excellent thermoprocessability. These properties can be attributed to the microphase crystalline and amorphous domain structure[3,4] resulting from phase separation between the aromatic diester blocks and the poly(alkylene oxide) blocks in the poly(ether ester). Applications of poly(ether ester)s include motor vehicle parts, flexible joints, cabling, and hosing. They have been investigated for use in medical devices[5] and in underwater hosing.[6] Commercial poly(ether ester)s generally contain a terephthalic acid/1,4-butanediol aromatic diester block and poly(ethylene oxide), poly(1,2-propyl-

ene oxide), or poly(tetramethylene oxide) (PTMO) as the poly(alkylene oxide) block.[3,7] Often some dimethyl isophthalate or dimethyl phthalate is included in the starting formulation with the dimethyl terephthalate in order to optimize the mechanical properties.

We reported previously[8] on improvements in oxidative and hydrolytic stability in a polyurethane, alternating-block copolymer by substituting a lower ether content poly(alkylene oxide) such as poly(decamethylene oxide) (PDMO), poly(octamethylene oxide), or poly(hexamethylene oxide) (PHMO) of similar molecular weight for a PTMO repeat block (commonly referred to as the soft segment). The work described herein continues the polyurethane study and adapts the approach to improved degradation resistance in poly(ether ester)s.[9] A series of poly(ether ester)s of controlled block copolymer structure consisting of a 1,4-butanediol chain extender, a terephthalate aromatic diester, and an approximately 1000 Da number average molecular weight ($\bar{M}_n$) poly(alkylene oxide) were prepared. The poly(alkylene oxide)s used were PTMO, PHMO, and PDMO. The novel poly(ether ester)s, the PTMO polyester, and a commercial control, Hytrel® 4056 were compared for their resistance to degradation in an aqueous oxidative environment at 37°C, boiling water buffered at pH 1 and 13, an oxygen stream at 200°C, and a nitrogen stream at 200°C.

The synthesis of a controlled and reproducible block copolymer structure by transition metal catalyzed transesterification at 250°C was more involved than the simple nucleophilic addition methods used to prepare the poly(ether urethane) materials. Attempts to increase molecular weight by variation of the macrodiol fraction relative to dimethyl terephthalate resulted in the synthesis of a series of poly(ether ester)s with aromatic diester repeat unit (hard segment) fractions of 25, 29, 37, and 51%. In each series, polyesters of PTMO and PHMO were prepared. In the 51% hard segment series, a PDMO polyester was also prepared. The $\bar{M}_n$ of the PTMO, PHMO, and PDMO soft segments were 980, 930, and 940 Da, respectively.

Molecular weights of the poly(ether ester)s were determined by viscometry and gel permeation chromatography (GPC). The alternating copolymer structure was verified by ^{1}H-NMR spectroscopy. Glass transition temperatures (T_g) and melting endotherms of the series were characterized using differential scanning calorimetry (DSC).

EXPERIMENTAL

A commercial PTMO–poly(ether ester) from Du Pont,[2] sold under the trade name Hytrel® 4056, was used as a control material.

Poly(alkylene oxide)s

The PTMO or poly(oxy-1,4-butanediyl)-α,ω-dihydroxy (1000 $\bar{M}_n$) was obtained from Du Pont under the trade name Terethane. The PHMO or poly(oxy-1,6-hexanediyl)-α,ω-dihydroxy (950 $\bar{M}_n$), and PDMO or poly(oxy-1,10-decanediyl)-α,ω-dihydroxy (960 $\bar{M}_n$) were synthesized from 1,6-hexanediol (BASF) and 1,10-decanediol (Aldrich), respectively, using a sulfuric acid catalyzed condensation reaction.[10]

Poly(ether ester) Synthesis

A typical commercial synthetic technique[11,12] was chosen to prepare the poly(ether ester) materials. This involved a two step bulk condensation reaction.[13] The first step (transesterification) was carried out at a temperature of 200°C with transesterification of a mixture of difunctional methyl ester, macrodiol, and diol (with a 50% stoichiometric excess of the diol). The transesterification was catalyzed by a transition metal complex.[14,15] The second step (polycondensation) was carried out by heating the mixture to between 250 and 270°C and the application of a vacuum (<0.1 Torr) to remove the excess of low molecular weight diol and hence produce chain extension. By minimizing the effects of degradative side reactions,[3,11,16] this synthesis technique can give high $\bar{M}_n$ products (ca. 10^5 Da).

The Pyrex glass laboratory reactor assembly used for the laboratory scale synthesis (Fig. 1) included a 500-mL reaction vessel (SVL 296-54) with a flanged lid (SVL 296-02) and an adapted quickfit vacuum stirrer fitting (ST20/2) with an IKA RW20-DZM (26-W output) stirrer. The reaction mixture was heated by immersion of the base of the reaction vessel in silicone oil to an oil level that was at least 1 cm above the reaction mixture. The silicone oil temperature was maintained using a thermocouple controlled Thermolyne Mirak™ 3-kW heater stirrer.

The poly(alkylene oxide) was predried by heating at 105°C for 15 h at 0.1 Torr. The poly(alkylene oxide), anhydrous 1,4-butanediol (Aldrich), dimethyl terephthalate (Aldrich), and the

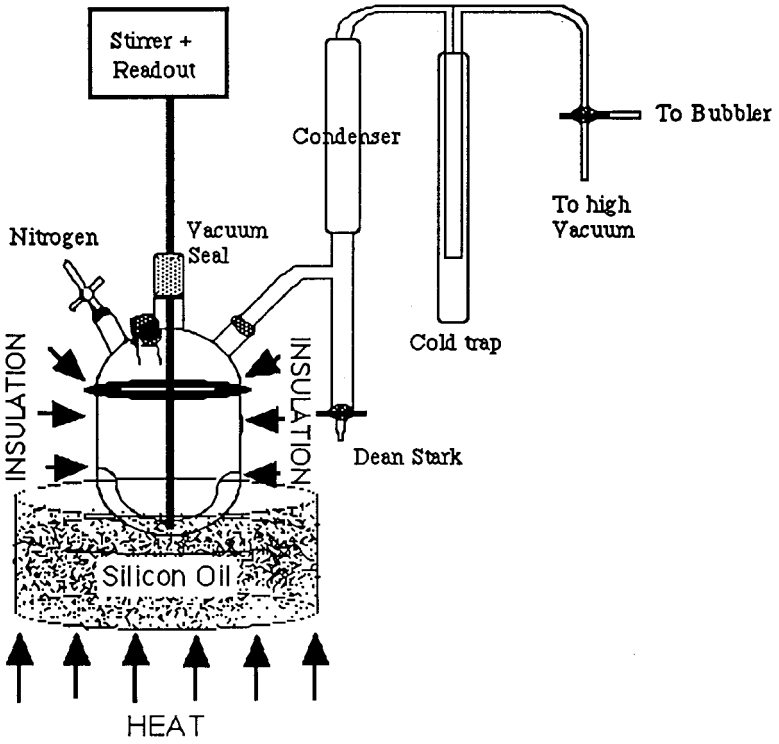

Figure 1 Schematic diagram of the 500-mL reaction vessel used to synthesize the poly(ether ester)s.

stabilizer *sym*-di-β-naphthyl-*p*-phenylenediamine (B. F. Goodrich) were added to the reaction vessel at 200°C under a continuous stream of nitrogen (see Table I for formulations). After 5 min of stirring, at which time the reaction mixture became molten, *n*-tetrabutyl titanate (Aldrich) catalyst was added. Methanol distillation commenced immediately and was generally complete within 20 min. The temperature was maintained for a further hour and then increased over 30 min to 250°C. The Dean Stark trap was emptied and the pressure was reduced slowly to 0.1 Torr. Distillation at reduced pressure and efficient stirring (200 rpm) was continued for a further 90–120 min. The end of the synthesis was signaled by a rapid increase in the viscosity of the reaction mixture causing stirring to cease. The reaction flask was opened, allowing the viscous slurry to be scraped (under N_2) from the bottom half of the flask onto Teflon™ sheeting at room temperature.

Portions from the resulting polymer slabs (dried for 24 h under a vacuum at 0.1 Torr and 60°C) were compression molded into 60 × 100 × 1 mm plaques at 200°C under an 8-tonne load.

Polymer Characterization

GPC was carried out at 140°C using a Waters 150C system with *m*-cresol as the mobile phase. The single ultrastyragel linear column was calibrated between 2×10^6 and 1×10^3 Da using monodisperse polystyrene standards. Viscometry was performed (×5 replicates) in dilute (0.1 g dL^{-1}) solution (*m*-cresol) at 30°C using an Ubbelohde capillary viscometer. ^{1}H-NMR (200 MHz) spectra were recorded on a Bruker AC200 FT-NMR spectrometer. The spectra were obtained from 2 to 4% (w/v) solutions in $CDCl_3$. DSC was performed between −150 and 250°C at 10°C min^{-1} using a Mettler DSC30S calorimeter. Samples for the DSC were preconditioned by heating at 70°C for 48 h at 0.5 Torr in a vacuum oven, heating at 80°C for 5 min in the DSC, and cooling at 10°C min^{-1} to −150°C. The DSC temperature was calibrated with hexane, water, and indium. Enthalpy change was calibrated from the melting endotherm of 5 mg of indium. Tensile analyses were performed with a crosshead speed of 500 mm min^{-1} on 1-mm thick punched dumbbell samples

(×5 replicates) using an Instron 4468 equipped with pneumatic grips and a 1-kN load cell. Samples were preconditioned under ambient conditions for at least 48 h before testing at room temperature. Shore hardness values were measured at 20°C with a calibrated A scale indentor by stacking five 1-mm thick moldings together on a flat hard surface.

Degradation Experiments

Resistance to hydrolytic degradation was examined by immersing dumbbell samples (×5 replicates) in pH 1 and 13 aqueous buffer solutions at 100°C for 144 h. A 50% solution of Solvay Interox H_2O_2 (aq) at pH 2 was used to test for resistance to oxidative degradation. Dumbbell samples (×5 replicates) were immersed in H_2O_2 (aq) solution for up to 48 h at 37°C. After treatment, samples were rinsed with water and dried at 60°C at 0.1 Torr for 12 h. Changes in mechanical properties due to the oxidative and hydrolytic treatments were determined by tensile analysis. The tensile indicator of resistance to degradation that was used was the ratio of the ultimate tensile strength (UTS) after exposure over the UTS before exposure (designated here as relative UTS). DSC measurements were carried out between 30 and 200°C at 10°C min^{-1} on 20-mg portions of degraded samples to examine for residual signs of oxidation.

Thermal degradation was determined using a Mettler TG50 Thermobalance. Poly(ether ester) disks (3-mm diameter and 1 mm thick) were dried to constant weight at 60°C at 0.1 Torr for 12 h and then heated in aluminum pans for up to 300 min at 200°C under a constant flow of oxygen or nitrogen at 20 mL min^{-1}. DSC analyses were also carried out on some of these degraded samples between −150 and 250°C at 10°C min^{-1}.

RESULTS AND DISCUSSION

Synthesis

The bulk synthesis of a poly(ether ester) to high molecular weight with good control of the alternating block copolymer structure is highly dependent on chemical reactor design. The features required[1,11,12] of an efficient reactor are uniform wall temperature control from 150 to 270°C, a good vacuum (<0.05 Torr), strong efficient mixing of the molten slurry, and a significant interfacial area between the evacuated headspace and the molten slurry.

Because a purpose-built reactor was not available for this work, the laboratory reactor assembly described previously was used. Buildup of condensate in the upper portion of the reactor was controlled by use of a hot air gun and glass wool insulation. The Teflon™ o-ring seals in the SVL vessel provided a good vacuum seal under the higher temperature of the second step. The ST20/2 quickfit vacuum fitting with silicone oil as the sealing fluid, although enabling a good vacuum, was subject to breakage under load. The power of the stirrer was only sufficient to maintain stirring up to a critical melt viscosity. Higher molecular weight polymer is likely to be achievable with a more powerful stirrer; however, there is a load limitation imposed by the ST20/2 vacuum seal. The stainless steel stirrer blade was fitted with a Teflon™ sleeve that was shaped to provide close contact with the glass surface at the base of the reactor. This ensured that the surface of the reactor was constantly wiped clean by the action of the blade rotation so that melt temperature uniformity in the viscous melt was maintained.

Preliminary syntheses sometimes experienced a slow transesterification in the first stage as evidenced by periods of methanol distillation exceeding 60 min. Slowness in this stage generally resulted in significant loss of dimethyl terephthalate by sublimation. It also resulted in materials with poor mechanical properties and low molecular weights. It was found that the extent of sublimation could be controlled by increasing the excess of 1,4-butanediol and also by minimizing deactivation of the catalyst[17–19] by ensuring dryness and low residual acidity in the reagents. Greater than 120-min exposure to the high temperature in the polycondensation step of the reaction was also detrimental to the mechanical properties and molecular weight of the poly(ether ester). In one preliminary formulation, containing a high fraction of poly(alkylene oxide), the reaction in the polycondensation stage was allowed to proceed for over 180 min. At 120 min a maximum in melt viscosity was achieved as seen by a very slow rotation of the stirrer. This slow stirring proceeded for up to 40 min, after which a change to a high rate of stirring indicated a lower melt viscosity. The resultant material was found to have poor mechanical properties and a low molecular

weight. These results are consistent with results of previously reported syntheses.[1,11]

Molecular Weight Determination

GPC provided the relative polystyrene molecular weight distributions for the poly(ether ester)s of PTMO (PTE), PHMO (PHE), and PDMO (PDE) materials PTE1, PHE2, PTE3, PHE3, PTE4, and PHE4 (Table II). The inherent viscosities of 0.1 g dL^{-1} *m*-cresol solutions at 30°C were determined for all materials (Table II). In the weight average molecular weight range ($\bar{M}_w$) of 22,000–123,000 $g^2\ mol^{-1}$, $\bar{M}_w$ can be shown to be a linear function of inherent viscosity (Fig. 2). For those samples for which it was not possible to perform GPC analyses, the linear relationship shown in Figure 2 provided a means of estimating the relative polystyrene $\bar{M}_w$.

The lower molecular weights measured in materials PHE2 and PTE3 are consistent with the presence of a significant level of end groups in the NMR spectra (Table III). For the remaining materials, molecular weight progressively declined from a $\bar{M}_w$ near 70,000 $g^2\ mol^{-1}$ at the 24% hard segment to a $\bar{M}_w$ near 45,000 $g^2\ mol^{-1}$ at the 51% hard segment (Table II). Assuming the polydispersity is between 2.0 and 2.5, then the $\bar{M}_n$ would be expected to similarly decline from near 40,000 to 20,000 g mol^{-1} in the same series.

Apart from PTE1, the molecular weights in this series are low when compared to those of commercial poly(ether ester)s. With improvements in the reactor design, possibly higher molecular weights could be achieved. However, for the purposes of this work, the molecular weight was sufficiently characterized and was sufficiently high to enable a controlled degradation analysis to be undertaken.

^{1}H-NMR Spectroscopy

The ^{1}H-NMR spectra of PTE5, PHE5, and PDE1 are depicted in Figure 3. Assignments of chemical shifts were determined from spectral analysis of the starting materials, splitting patterns, and signal areas. The ^{1}H-NMR spectra are consistent with the structures depicted in **1a, 1b,** and **1c.**

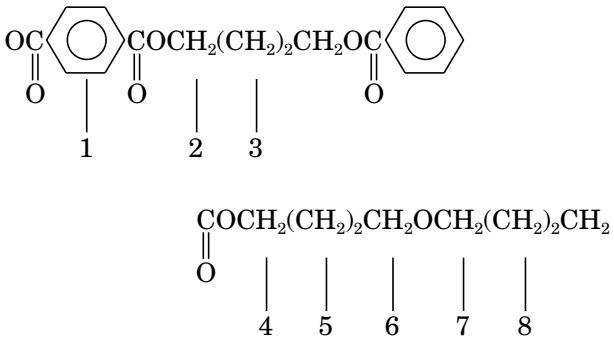

1a

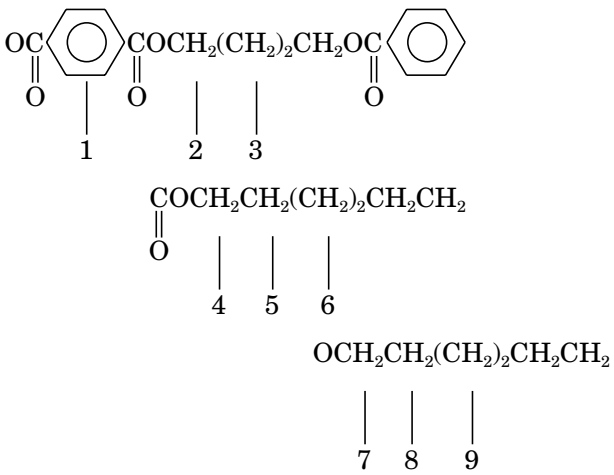

1b

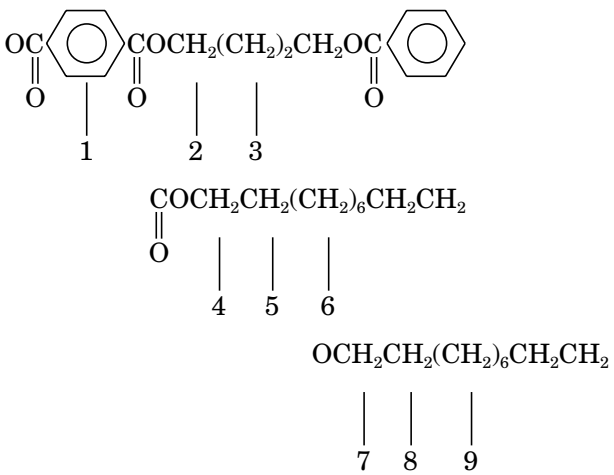

1c

The ^{1}H-NMR integrated peak areas of hydrogens 1, 2, and 7 were used to calculate the mole ratios of the dicarboxylate : diol : macrodiol in the poly(ether ester)s and hence to determine the mass percentages of the hard segment (Table III). The presence of a singlet at δ3.88 ppm in the PHMO

Table I Starting Material Molar Ratios for Polyester Synthesis

	Diester + Diol + Macrodiol (Rel. Molar Amount in Parens)			Stabilizer + Catalyst	
Formulation	*A* (g)	*B* (g)	*C* (g)	*D* (g)	*E* (mL)
ET1 (**25**)	22.7 (1.8)	12.0 (2.1)	63.5 (1.0)	0.15	0.3
PHE1 (**25**)	22.7 (1.8)	17.0 (2.8)	63.7 (1.0)	0.15	0.3
PTE2 (**29**)	28.2 (2.2)	16.0 (2.7)	67.0 (1.0)	0.15	0.3
PHE2 (**29**)	28.0 (2.2)	12.0 (2.0)	63.7 (1.0)	0.15	0.3
PTE3 (**29**)	27.8 (2.2)	16.0 (2.7)	67.0 (1.0)	0.15	0.3
PHE3 (**29**)	28.0 (2.2)	16.0 (2.7)	63.7 (1.0)	0.15	0.3
PTE4 (**37**)	30.3 (2.9)	19.7 (4.0)	54.0 (1.0)	0.15	0.3
PHE4 (**37**)	30.5 (2.9)	19.6 (4.0)	51.3 (1.0)	0.15	0.3
PTE5 (**51**)	103.1 (4.9)	55.0 (5.6)	107.7 (1.0)	0.30	0.6
PHEE5 (**51**)	103.4 (4.9)	54.4 (5.3)	107.9 (1.0)	0.30	0.6
PDE1 (**51**)	37.6 (4.8)	19.6 (5.3)	39.2 (1.0)	0.10	0.22

PTE, PHE, and PDE are poly(ether ester)s of poly(tetramethylene oxide), poly(hexamethylene oxide), and poly(decamethylene oxide), respectively. *A* is the mass of 1,4-butanediol, *B* is the mass of dimethyl terephthalate, *C* is the mass of poly(alkylene oxide), *D* is the mass of symdi-β-naphthyl-*p*-phenylenediamine, and *E* is the volume of *n*-tetrabutyl titanate.

based materials PHE2 and PHE3 is consistent with residual methoxy end groups and incomplete transesterification in the first step of the polymerization. A small triplet at δ 3.63 ppm in the PTMO based materials PTE2, PTE3, and PTE5 and the PHMO based material PHE5 (Table III) is consistent with residual terminal hydroxy groups α to the methylene hydrogens, suggesting either poor chain extension in the polycondensation stage or the presence of residual 1,4-butanediol.

The ^{1}H-NMR spectrum of Hytrel® 4056 was also recorded. The presence of small peaks at 8.68, 8.24, and 8.00 ppm and a triplet at 7.53 ppm are consistent with a small component of isophthalic acid. The remaining peaks of the NMR spectrum identified Hytrel® 4056 as being predominantly composed of PTMO ($\bar{M}_n$ = 790 Da), terephthalic acid, and butanediol. The mole ratio of terephthalic acid : butanediol : PTMO was determined as 3.4 : 3.5 : 1. The butanediol/terephthalic acid hard segment fraction was determined to be at least 49%.

Analysis of the NMR spectra indicates (Table III) that the variation in hard segment fraction in nominal 24, 29, 37, and 51% poly(ether ester) series fractions is less than 4% of the hard seg-

Table II Polyester Molecular Weights

Material	$\bar{M}_n$ (g mol^{-1})	$\bar{M}_w$ (g^2 mol^{-1})	$\bar{M}_w/\bar{M}_n$ (g)	η_{inh} (dL g^{-1})
Hytrel 4056	44700	95,100	2.1	1.48
PTE1 (**25**)	68170	123,000	1.8	1.78
PHE1 (**25**)	—	[68,000]	—	1.10
PTE2 (**29**)	—	[57,000]	—	0.97
PHE2 (**29**)	8200	21,700	2.6	0.52
PTE3 (**29**)	9100	26,600	2.9	0.58
PHE3 (**29**)	13400	42,300	3.2	0.81
PTE4 (**37**)	24700	63,100	2.6	1.04
PHE4 (**37**)	16940	48,470	2.9	0.81
PTE5 (**51**)	—	[48,000]	—	0.85
PHE5 (**51**)	—	[46,000]	—	0.82
PDE1 (**51**)	—	[38,000]	—	0.73

Molecular weights by GPC and viscometry. The molecular weights for samples PHE1, PTE2, PTE5, and PDE1 were characterized by viscometry alone with the values in brackets estimated from Figure 2.

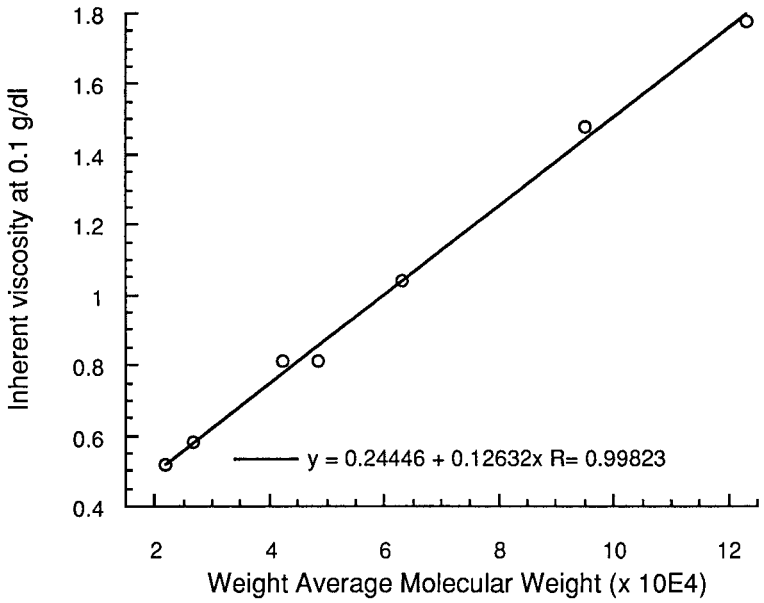

Figure 2 Weight average molecular weight ($\bar{M}_w$) plotted against inherent viscosity for the poly(ether ester)s.

ment fraction and is independent of soft segment type. The molar ratio of the terephthalic acid/butanediol/macrodiol in the product poly(ether ester)s is only very slightly different from the molar ratio expected from the starting material (Table I).

DSC

The DSC thermograms for the bulk of the produced materials (PTE1, PHE1, PTE2, PHE3, PTE4, PHE4, PTE5, PHE5, and PDE1) are shown in Figure 4. The position of the small hard segment peak at 92.5°C is controlled by the 80°C annealing treatment prior to running the differential scan (see Materials and Methods). The main features in the thermograms are the polyether glass transitions at subambient temperatures, the significant soft segment domain polyether paracrystalline melting peaks below 70°C, and the hard segment domain (aromatic diester) paracrystalline melting peaks above 70°C. The significant crystallinity in both hard and soft segment domains is indicative of a high degree of phase separation.

Table III ^{1}H-NMR Structural Analysis of Experimental Polyesters

Material	*m*(diacid) : *m*(diol) : *m*(macrodiol)	Mass % Hard Segment	OCH_3 End Groups	$HOCH_2$ End Groups
PTE1 (**25**)	1.65 : 0.65 : 1.00	23.0	Not detected	Not detected
PHE1 (**25**)	1.75 : 0.75 : 1.00	25.0	Not detected	Not detected
PTE2 (**29**)	2.10 : 1.10 : 1.00	29.0	Not detected	Present
PHE2 (**29**)	2.00 : 1.00 : 1.00	28.0	Present	Not detected
PTE3 (**29**)	2.10 : 1.10 : 1.00	29.0	Not detected	Present
PHE3 (**29**)	2.20 : 1.20 : 1.00	30.0	Present (weak)	Not detected
PTE4 (**37**)	2.85 : 1.85 : 1.00	36.0	Not detected	Not detected
PHE4 (**37**)	2.85 : 1.85 : 1.00	37.0	Not detected	Not detected
PTE5 (**51**)	4.90 : 3.90 : 1.00	50.7	Not detected	Present
PHE5 (**51**)	4.70 : 3.70 : 1.00	50.7	Not detected	Present (weak)
PDE1 (**51**)	4.70 : 3.70 : 1.00	50.6	Not detected	Not detected

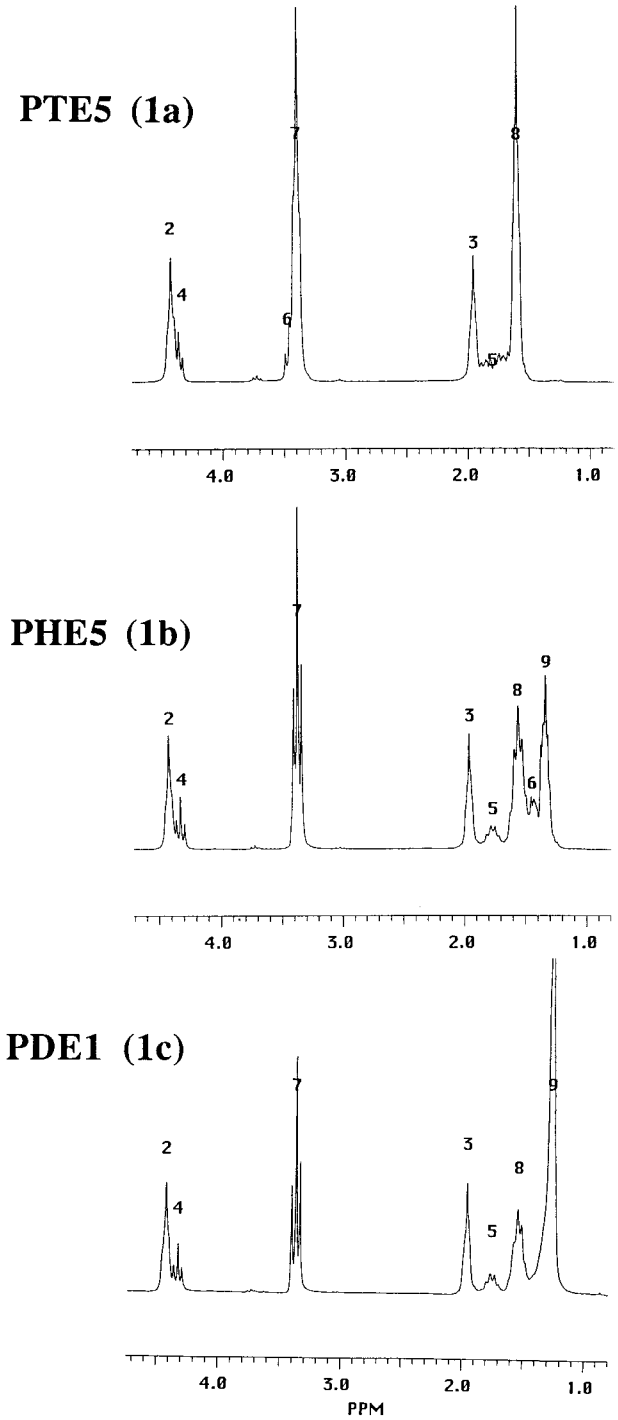

Figure 3 ^{1}H-NMR spectra of PTE5, PHE5, and PDE1 from δ0.75 to 4.75 ppm. The one peak (singlet) at δ8.09 ppm not shown results from the four terephthalic acid hydrogens (peak 1 in structures **1a, 1b,** and **1c**).

In contrast to the PHMO and PDMO polyester materials, the PTMO thermograms exhibit a cold crystallization due to a slower rate of crystallization in the PTMO (seen on cooling at 10°C min^{-1} from 80 to −150°C). Table IV lists the main characteristics of the DSC analyses.

The DSC thermograms demonstrate similarity in the degree of phase separation and hard segment domain crystallinity between poly(ether ester)s of PTMO, PHMO, and PDMO at the same fractions of the hard segment. The most relevant parameters (Table IV) are the change in heat capacity per mass of segment type (ΔC_p^*) in the soft segment glass transition region and the enthalpy changes per mass of segment type (ΔH^*) and the peak melting temperatures (P_k) in the crystalline melting endotherms of both the hard and soft segment regions. Increases in P_k, ΔC_p^*, and ΔH^* with changes in hard segment fraction for both the hard and soft domains indicate increased phase separation while the opposite indicates phase mixing (Fig. 5). Changes occurring in the hard segment domain ΔH^* and P_k with increasing mass fraction of the hard segment are also indicative of increasing block size (from a mean

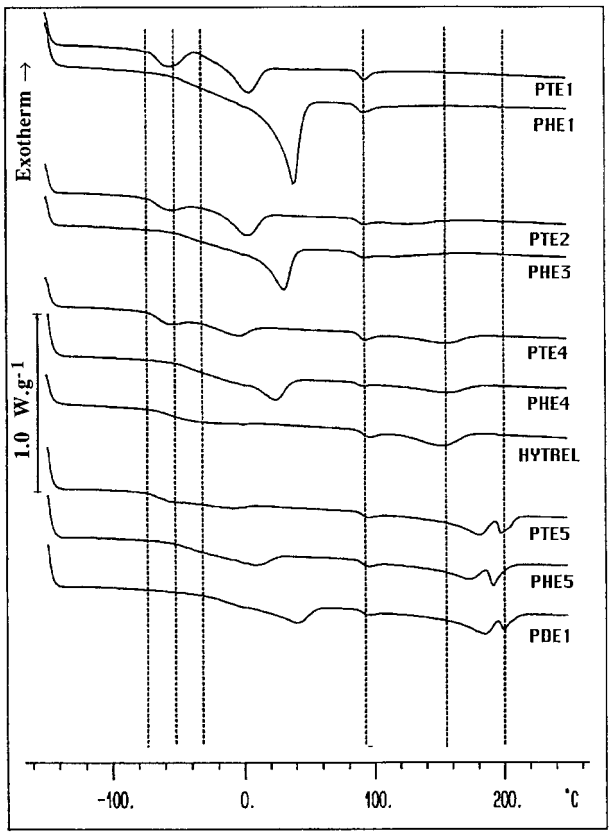

Figure 4 Differential scanning calorimetry (DSC) thermograms of PTE1, PHE1, PTE2, PHE3, PTE4, PHE4, HYTREL® 4056, PTE5, PHE5, and PDE1.

Table IV DSC Analysis of Experimental Polyesters

	Subambient (Soft Segment Region)						Hard Segment	
	Glass Transition Temperature (T_g) Change				Crystalline Melting		Crystalline Melting	
Materials	Onset (°C)	Midpt (°C)	Endpt (°C)	ΔC_p*[a] (J/gK)	ΔH*[a] (J/g)	P_k (°C)	ΔH*[a] (J/g)	P_k (°C)
PET1 (**25**)	−75	−66	−61	0.65	21.4	3.7	13.5	92.5
PHE1 (**25**)	−54	−26	−0.5	0.80	53	35.9	13.2	92.5
PET2 (**29**)	−75	−66	−59	0.62	22.5	2.2	38	125
PHE3 (**29**)	−54	−26	−0.5	0.64	45	30.1	38	118
PTE4 (**37**)	−74	−66	−59	0.59	11	−4.3	47	154.1
PHE4 (**37**)	−54	−49	−23	0.65	29.5	23.8	44	154.0
PTE5 (**51**)	−74	−66	−57	0.47	6.1	−8.9	69	179.3 197.7
PHE5 (**51**)	−54	−42	−30	0.49	22.3	7.8	61	171.1 191.0
PDE1 (**51**)	−26	−15	−3.5	0.32	29.5	39.4	69	184.4 199.4
Hytrel®	−68	−55	−41.5	[0.33]	[0.8]	−1.1	[22.0]	148.5

[a] With the exception of Hytrel® (% hard segment unknown), per mass change was determined as per mass change of particular block type (i.e., hard or soft depending on melting region).

1.7 terephthalic acid units/block to 4.8). Such an increase results in a more highly ordered crystalline domain and a subsequently higher melting point. It can be seen that ΔH* increases from 13 to 70 J/g and P_k increases from 100 to 200°C as hard segment fraction is increased through 24–51%.

Variations in soft segment midpoint and endpoint glass transition temperatures (T_g) cannot be interpreted unambiguously because they are both significantly perturbed by the soft segment crystalline melting endotherms. The onset of the soft segment glass transition is outside the range of crystalline melting effects and does provide corroboration of the degree of phase separation. Inability to detect any difference in soft segment onset glass transition for the PTE polyesters (T_g onset = −75°C) and the PHE polyesters (T_g onset = −54°C) with a change in the fraction of the hard segment from 24 to 51% further demonstrates the relatively poor phase mixing between the poly(ether ester) soft and hard segments. Evidence of a small level of phase mixing is reflected in a decrease in the ΔH* and P_k in the soft segment domains with an increase in the percent of hard segments (Fig. 5). A significantly higher onset glass transition for the Hytrel® PTMO (−68°C) compared to the PTE PTMO (−75°C) in conjunction with the insignificant PTMO melting endotherm for the Hytrel® demonstrate a higher level of phase mixing in this polymer. This phase mixing is likely due to the presence of a disrupting hard segment comonomer such as isophthalic acid (see NMR discussion).

Tensile and Hardness Characterization

The Shore A hardness and tensile properties of the different polyesters are listed in Table V. The PTE polyesters show a gradual increase in hardness with an increasing fraction of the hard segment from 60A to 95A while the PHE polyesters show only minimal hardness change (90A to 95A). It would appear that the reason for this difference is the significant fraction of the soft segment crystallinity in each type of polyester combined with their respective melting temperatures (Table IV) relative to ambient temperature (20°C). For the PTE polyesters, the melting temperatures are between 3.7 and −8.9°C while for the PHE polyesters the melting temperatures are mostly above ambient temperature (35.9, 30.1, 23.8, and 7.8°C).

A better indicator of the effect of crystallinity in the hard and soft segments is the Young's modulus. It can be seen for 25 and 29% hard segment

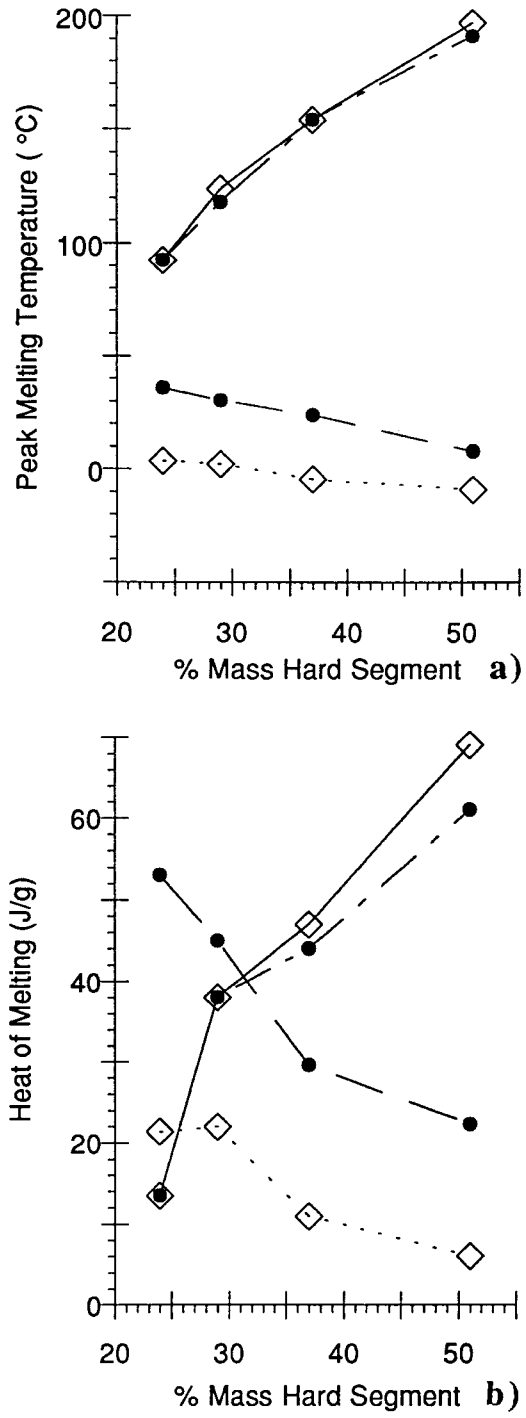

Figure 5 Change in (a) peak melting temperatures and (b) heats of melting/(mass of segment type) with change in percent mass of hard segment for (◇) PTE and (●) PHE poly(ether ester)s. Hard segment change is depicted for (—) PTE polyesters and (– – –) PHE polyesters. Soft segment change is depicted for (---) PTE polyesters and (– – –) PHE polyesters.

fractions that the PTE materials have significantly lower Young's modulus compared to their equivalent hard segment fraction PHE materials. However, for the 38 and 51% hard segment fraction materials, the difference in Young's modulus between PTE and PHE materials becomes more dependent on hard segment crystallinity (Table IV) and at 51% hard segment fraction the modulus of PTE5 is greater than PHE5. PDE1 has the highest Young's modulus that again appears to be due to significant hard segment crystallinity.

UTS is related to hard segment crystallinity, degree of phase separation, and polymer molecular weight. The superior UTS (and ultimate percent elongation) of PTE displayed between the same hard segment fraction pairs of PTE1 and PHE1, PTE2 and PHE3, and PTE4 and PHE4 is predominantly related to the higher molecular weights of the PTMO polyesters in these pairings. PTE5, PHE5, and PDE1 all have similar UTS and ultimate percent elongation due to a similarity in polymer molecular weight. Both PHE2 and PTE3 exhibited very poor mechanical properties due to their low molecular weights ($\bar{M}_w$ = 22,000 and 27,000 g^2 mol^{-1}, respectively). The consistently low tensile properties of the polyesters synthesized in this work most probably result from the combination of relatively low molecular weights (the M_w having a mean value near 50,000 g^2 mol^{-1}) and a sharp phase separation between the poly(alkylene oxide) and the aromatic diester domains.

Polyester Stability

Exposure to Hydrolysis at 100°C at pH 1 and 13

The results of hydrolysis testing of Hytrel® 4056, PTE4, PHE4, PTE5, and PDE1 in pH 1 and pH aqueous buffer solutions at 100°C for 144 h are shown in Figure 6. The effect of increasing the fraction of the hard segment is to increase the relative hydrolytic stability; hence PTE4 with 37% mass fraction of the hard segment is considerably less stable than PTE5 with a hard segment mass fraction of 51%. Hydrolytic stability also increases with reduction in the ratio of ether to methylene units; hence with the same fraction hard segment, PHE4 is substantially more hydrolytically stable than PTE4, and PDE1 is more hydrolytically stable than PTE5.

Exposure to 50% Hydrogen Peroxide at 37°C

Samples (PTE1, PHE1, PTE4, PHE4, PTE5, PDE1, and Hytrel® 4056) were tested for their

Table V Durometer Shore A Hardness and Tensile Properties of Experimental Polyesters

Materials	Shore A[a] Hardness	Ultimate Tensile Strength (MPa)	Ultimate Elongation (%)	Young's Modulus (MPa)	Stress at 100% Elong. (MPa)
PTE1 (**25**)	60	12 ± 0.3	1280 ± 30	1.2	2.1 ± 0.15
PHE1 (**25**)	90 (28)	3.7 ± 0.1	73 ± 7	12.6 ± 0.2	—
PTE2 (**29**)	75 (17)	4.2 ± 0.1	348 ± 25	10.8 ± 0.1	3.5 ± 0.05
PHE2 (**29**)[b]	95 (40)	—	—	—	—
PTE3 (**29**)[b]	70	—	—	—	—
PHE3 (**29**)	90 (28)	3.7 ± 0.05	117 ± 32	14.4 ± 1.2	3.6 ± 0.3
PTE4 (**37**)	90 (30)	10.4 ± 0.3	330 ± 25	28.1 ± 0.1	8.7 ± 0.1
PHE4 (**37**)	90 (30)	8.1 ± 0.2	168 ± 5	27.9 ± 0.5	7.8 ± 0.1
PTE5 (**51**)	95 (42)	12.9 ± 0.1	165 ± 6	94 ± 7	12.8 ± 0.2
PHE5 (**51**)	95 (40)	12.1 ± 0.3	226 ± 11	60 ± 2	11.7 ± 0.3
PDE1 (**51**)	95 (42)	13.8 ± 0.6	143 ± 17	123 ± 9	12.0 ± 0.5
HYTREL®	95 (42)	30.1 ± 2.4	775 ± 60	42 ± 4	10.6 ± 0.02

[a] Shore D hardness for the harder materials in parentheses.
[b] Dumbells failed in clamp.

resistance to degradation in 50% hydrogen peroxide solution at 37°C. After 24-h exposure to the oxidative conditions, only samples PHE1, PHE4, and PDE1 remained intact and PDE1 exhibited 85% of its original UTS and PHE2 exhibited 81%. All the PTMO based polyesters exhibited signs of digestion, fragmentation, and severe embrittlement under these conditions. Sample PHE1 was exposed to the hydrogen peroxide for 48 h with a resultant loss of 68% of its mechanical properties. PHMO and PDMO based polyesters were clearly superior to PTMO based polyesters in terms of resistance to hydrogen peroxide degradation.

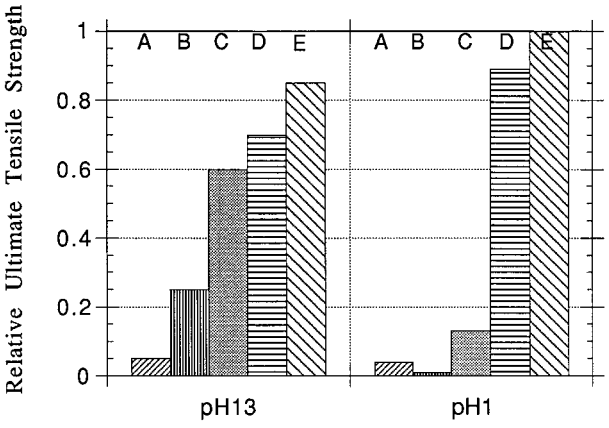

Figure 6 Histograms of the relative ultimate tensile strength (the ratio in UTS after and before hydrolytic exposure) of (A) Hytrel® 4056, (B) PTE4, (C) PHE4, (D) PTE5, and (E) PDE1 in pH 1 and 13 aqueous buffer solutions at 100°C for 144 h.

The mechanism of degradation in hydrogen peroxide was tested by washing the degraded samples in water to remove residual hydrogen peroxide and drying under a vacuum at 60°C for 24 h before performing a DSC experiment. A large exotherm (up to 500 J/g) was observed with an onset temperature of 110°C. Such behavior is consistent with the presence of organic peroxide species and substantial oxidative degradation of the polyesters.

Thermal Degradation by Exposure to 200°C

Significant thermal degradation was observed in all the polyester materials when they were exposed to 200°C for periods up to 300 min. The mass loss thermograms for a range of the new polyester materials (PTE1, PHE1, PTE2, PHE3, PTE4, PHE4, PTE5, PHE5, and PDE1) are shown in Figure 7. The thermogravimetric technique measures loss of volatile degradation products at elevated temperature. A full interpretation of thermogravimetric change would normally be dependent on complementary analyses of the degradation products by techniques such as end group analysis, mass spectroscopy, NMR, and/or infrared spectroscopy. However, our work only intended to ascertain relative stabilities between materials designed to be essentially identical except for the ether oxygen content of the macrodiol.

The main features of the thermograms shown in Figure 7 are

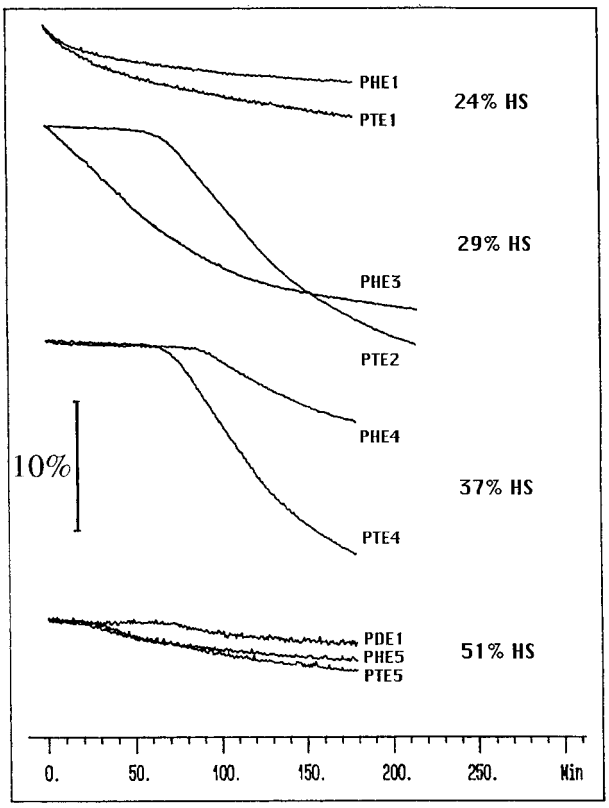

Figure 7 Fractional mass loss thermograms at 200°C (under O_2 flow) for up to 200-min thermal exposure for samples PHE1, PTE1, PHE3, PTE2, PHE4, PTE4, PDE1, PHE5, and PTE5. HS, Hard segment.

- the presence or absence of induction periods lasting up to 90 min;
- an initial rapid mass loss declining to a plateau level of ca. 7, 15, 15, and 4% mass loss after 180 min for 24, 29, 37, and 51% hard segment polyester fractions, respectively;
- rate of mass loss across a series with the same mass fraction of hard segment, dependent on the ratio of ether to methylene units in the soft segment with the rate and extent of mass loss increasing in the order PDE < PHE < PTE; and
- the samples exhibited the same mass loss behavior independent of the gas stream environment.

The presence of substantial induction periods in samples PTE2, PHE4, PTE4, and PDE1 may possibly be attributed to the presence of residual quantities of the antioxidant *sym*-di-β-naphthyl-*p*-phenylenediamine[3] or differences in residual metal catalyst. The differences in the plateau levels at different hard segment fractions is difficult to attribute to any one factor due to the higher level of mass loss in the intermediate mass fractions and a low level of mass loss experienced by the high (51%) and low (24%) mass fractions. Significant crystalline structure in the higher melting polyesters (near 200°C) and relative differences in thermal stability between the soft segment and hard segment components may be responsible for this observed behavior.

The factors most likely to affect mass loss from the poly(ether ester)s at 200°C are

- the partial pressure of degradation products at 200°C,
- permeability of degradation products in the bulk,
- the ratio of polymer surface area to polymer volume,
- degradation reactions that might produce crosslinking and/or chain extension, and
- inherent resistance to thermal degradation in the polymer.

Consideration of the degradation of the pure components of the poly(ether ester)s at elevated temperature suggests that the partial pressure of the degradation products is unlikely to play an important role. Poly(butylene terephthalate) degrades at elevated temperature to yield butadiene, terephthalic acid, and unsaturated terephthalic esters.[16,20] The thermal degradation of poly(hexamethylene terephthalate) and poly(decamethylene terephthalate) were shown[21] to produce carbon dioxide, 5-hexene-1-ol, 1,5-hexadiene, and dodecatriene for poly(hexamethylene terephthalate) and carbon dioxide and 9-decene-1-ol for poly(decamethylene terephthalate).

Thermal degradation of the macrodiols PTMO, PHMO, and PDMO at 200°C results in at least 80% mass loss of all the polyols within 20 min. The relative rate of mass loss in the pure macrodiols increases as the ratio of ether to methylene units increases: PDMO < PHMO < PTMO.

In the absence of extensive crosslinking, the degradation products from the different poly(ether ester)s would be expected to volatilize relatively quickly (at least 50% mass loss within 20 min) at 200°C from 20-mg samples under gas flow. Because the rate of mass loss that occurs in the poly(ether ester)s is considerably less than the

slowest rate of volatilization, it is possible to conclude that volatilization is not the limiting step determining the rate of mass loss in the poly(ether ester).

To test for crosslinking, samples degraded under oxygen were removed from their sample container and placed in chloroform. It was found that chloroform, which normally dissolves the poly(ether ester)s, caused the materials to quickly fragment into small, slightly swollen, red to dark, crescent-shaped gel particles. When the chloroform was allowed to dry, it left a single residue of the red gel particles. Samples that were degraded in a nitrogen atmosphere were similarly treated. They broke down more slowly to a slightly colored solution and a dispersion of fine, dark, nonswollen particles. In this case, when the chloroform was allowed to dry, it left nearly equal parts of insoluble particles and a soluble polymer residue.

Some DSC analyses were run on the thermally degraded samples treated under both nitrogen and oxygen. It was found that the oxygen treated samples, although possessing the normal soft segment glass transition, had no detectable soft segment crystalline melting peaks whereas the nitrogen treated samples did have a normal soft segment crystalline melting peak.

These results indicate that samples heated under nitrogen possess significantly less crosslinking than those heated under oxygen.

The presence of crosslinking in the thermally degraded samples may influence the mass loss behavior because significant crosslinking would be expected to retard diffusion of volatiles to the surface. Also, with significant crosslinking it would be expected that degradation products from the PDE materials would be retarded more effectively than those from a PTE material and hence the rate of mass loss for a PDE polyester would be less than that expected for a PTE polyester. If crosslinking and diffusion controlled rate of mass loss, then any significant change in crosslinking should produce a subsequent change in the rate of mass loss. The absence of such a change when performing the isothermal experiments under different gaseous environments that cause substantial differences in crosslinking indicates that diffusion is not the significant limiting step determining the rate of mass loss.

Therefore, if volatilization and diffusion processes do not determine the rate of mass loss under controlled surface to volume conditions, then the rate of polymer degradation must be the rate determining step. These thermogravimetric results indicate that polymer thermal stability is substantially enhanced by a reduced fraction of ether linkages per methylene unit in the soft segment with stability promoted in the order PDMO > PHMO > PTMO.

CONCLUSIONS

A series of poly(ether ester) block copolymers of very similar morphology at different hard segment fractions of 24, 29, 37, and 51% with poly(alkylene oxide) soft segment blocks of PTMO ($\bar{M}_n$ = 1000 Da), PHMO ($\bar{M}_n$ = 950 Da), or PDMO (only at a 51% hard segment fraction) ($\bar{M}_n$ = 960 Da) were synthesized. In the investigation of their hydrolytic stability in pH 1 and 13 solutions at reflux (144 h) and oxidative stability in 50% solution of hydrogen peroxide (37°C) it was found that resistance to the different modes of degradation increases with an increased ratio of methylene to ether units: PTMO < PHMO < PDMO. An increasing fraction of the hard segment was found to significantly increase the poly(ether ester) resistance to hydrolysis.

In the thermal degradation at 200°C, there was a similar order of stability enhancement: PTMO < PHMO < PDMO.

REFERENCES

1. J. R. J. Wolfe, in *Block Copolymers: Science and Technology,* D. J. Meier, Ed., Harwood Academic Publishers, New York, 1983, p. 145.
2. *HYTREL® Product and Properties Guide* 1, Du Pont Polymers, Wilmington, DE, 1991.
3. R. K. Adams and G. K. Hoeschele, *Thermoplastic Polyester Elastomers,* Hanser, New York, 1987, p. 163.
4. D. J. Meier, in *Thermoplastic Elastomers: A Comprehensive Review,* N. R. Legge, G. Holden, and H. E. Shroeder, Eds., Hanser Publishers, New York, 1987, p. 269.
5. W. L. J. Hinrichs, J. Kuit, H. Feil, C. R. H. Wildevuur, and J. Feijen, *Biomaterials,* **13,** 585 (1992).
6. J. Hodgkin, *Environmental Degradation Mechanisms in Commercial Thermoplastic Polyesters,* Pacific Polymer Federation, Koloa, Kauai, HI, 1995, p. 305.
7. R. P. Quirk, M. A. Alsamarraie, and W. Schoenmaker, in *Handbook of Elastomers: New Develop-*

ments and Technologies, A. K. Bhowmick and H. L. Stephens, Eds., Marcel Dekker, New York, 1988, p. 341.
8. P. A. Gunatillake, G. F. Meijs, R. C. Chatelier, S. J. McCarthy, A. Brandwood, and K. Schindhelm, *J. Appl. Polym. Sci.,* **46,** 319 (1992).
9. S. J. McCarthy and G. F. Meijs, Int. Pat. WO 95/29201 (1994).
10. P. A. Gunatillake, G. F. Meijs, R. Chatelier, D. M. McIntosh, and E. Rizzardo, *Polym. Int.,* **27,** 275 (1992).
11. W. K. Witsiepe, in *Polymerization Reactions and New Polymers,* N. Platzer, Ed., American Chemical Society, Washington, DC, 1973, p. 39.
12. J. R. J. Wolfe, *Rubber Chem. Technol.,* **50,** 688 (1977).
13. F. Pilati, in *Step Polymerization,* G. C. Eastmond, A. Ledwith, S. Russo, and P. Sigwalt, Eds., Pergamon Press, New York, 1989, p. 275.
14. A. Fradet and E. Marechal, *Adv. Polym. Sci.,* **43,** 51 (1982).
15. J. Otton, S. Ratton, G. D. Markova, K. M. Nametov, V. I. Bakhmutov, L. I. Komarova, S. V. Vinogradova, and J. V. Korshak, *J. Polym. Sci.: Part A: Polym. Chem.,* **26,** 2199 (1988).
16. H. Zimmerman, *Degradation and Stabilization of Polyesters,* Applied Science, New York, 1984, p. 79.
17. F. Pilati, P. Manaresi, B. Fortunato, A. Munari, and V. Passalacqua, *Polymer,* **22,** 799 (1981).
18. F. Pilati, A. Munari, P. Manaresi, and V. Bonora, *Polymer,* **26,** 1745 (1985).
19. C. C. Walker, *J. Polym. Sci., Polym. Chem. Ed.,* **21,** 623 (1983).
20. V. Passalacqua, F. Pilati, V. Zamboni, B. Fortunato, and P. Manaresi, *Polymer,* **17,** 1044 (1976).
21. G. Rafler, J. Blaesche, B. Moeller, and M. Stromeyer, *Acta Polym.,* **32,** 608 (1981).